Modeling and Simulation of Tympanic Membrane Vibration

Multimodal Modeling and Real-Time 3D Simulation of Tympanic Membrane Vibration

Karim Mohamed El-Sayed | 91240578, Mona Elkhouly | 91241075, Khadija Zakaria | 91240965, Hana Gamal | 91240843, Manar Saed | 91240785, Farah Yehya | 91240560, Ibrahim Abdelqadeer | 91240056

***Abstract*—The tympanic membrane plays a key role in hearing by converting acoustic pressure into mechanical vibration. In this project, the free vibration behavior of the tympanic membrane is studied using analytical, numerical, and data-driven approaches, supported by three-dimensional simulation. The membrane is modeled as a sectorial annulus under uniform tension, and its motion is governed by a two-dimensional wave equation in polar coordinates. An analytical solution is derived using separation of variables, leading to a Bessel differential equation that yields closed-form expressions for natural frequencies and vibration mode shapes. A numerical solution based on the finite difference method is also implemented, resulting in an eigenvalue problem from which multiple vibration modes are obtained and visualized as three-dimensional surfaces. Modal indices are identified by analyzing nodal circles and nodal diameters. In addition, a physics-informed neural network (PINN) is developed to solve the governing partial differential equation by embedding physical constraints into the learning process. Finally, a real-time three-dimensional simulation of tympanic membrane vibration is implemented in the Unity game engine, where sound excitation drives membrane deformation according to the underlying model. The results show consistent qualitative agreement across all approaches.**

***Index Terms*—Bessel Function, Free vibration Model,Tympanic Membrane, PINNs, Unity Simulator.**

I. Introduction to The Problem

AUDITORY system is a highly sensitive and mechanically complex structure responsible for converting acoustic pressure waves into neural signals perceived as sound. A critical component of this system is the **tympanic membrane (TM)**, which serves as the primary interface between airborne sound in the external ear canal and mechanical vibrations transmitted through the middle ear ossicular chain. The vibratory behavior of the tympanic membrane directly influences sound transmission efficiency and, consequently, hearing performance. Damage or alteration of the membrane can significantly impair sound transmission, and although surgical procedures such as myringoplasty aim to restore its function, clinical outcomes often rely on empirical experience due to the difficulty of accurately modeling middle-ear mechanics. To better understand tympanic membrane mechanics, previous studies have employed numerical approaches, particularly finite element methods, to analyze vibration behavior under acoustic excitation. While these methods provide detailed spatial information, they require significant computational resources and rely on numerous assumptions regarding material properties and boundary conditions. Analytical modeling offers a complementary perspective by reducing model complexity and providing closed-form solutions that clarify the underlying physical mechanisms governing membrane vibration.

Under appropriate assumptions, the tympanic membrane can be idealized as a thin, flexible membrane subjected to uniform in-plane tension and fixed boundaries. Modeling the membrane as a sectorial annulus enables the formulation of its free vibration behavior using a two-dimensional wave equation in polar coordinates. Applying separation of variables reduces the governing equation to a Bessel differential equation, from which natural frequencies and vibration mode shapes can be derived analytically.

Building on this theoretical framework, the present work studies the free vibration of the tympanic membrane using analytical, numerical, and data-driven approaches. A finite difference method is implemented to numerically solve the governing equation and compute multiple vibration modes, which are identified through nodal circles and nodal diameters. In addition, a physics-informed neural network is developed to solve the same problem by embedding physical constraints into the learning process. Finally, a real-time three-dimensional simulation is created to visualize tympanic membrane vibration under sound excitation. Together, these approaches provide a consistent and comprehensive understanding of tympanic membrane vibration behavior.

II. LITERATURE REVIEW

A. Analytical Free Vibration Modeling of the Tympanic Membrane[1]

Analytical modeling of the tympanic membrane has been pursued to provide physical insight into its vibratory behavior while avoiding the computational complexity associated with full numerical simulations. Unlike comprehensive finite element models that incorporate multiple anatomical structures, analytical approaches typically rely on simplified geometries and assumptions to derive closed-form solutions for natural frequencies and mode shapes.

A notable contribution in this area was presented by Wu et al. **wu2016free**, who developed a free vibration model of the tympanic membrane by idealizing it as a sectorial annulus membrane under uniform in-plane tension. Based on anatomical and mechanical considerations, the tympanic membrane was assumed to be thin, flexible, and incapable of resisting bending or shear deformation, with fixed boundary conditions imposed by the annular ligament. Under these assumptions, the membrane motion was governed by a two-dimensional wave equation expressed in polar coordinates.

Using the method of separation of variables, the governing equation was reduced to a Bessel differential equation, enabling the derivation of analytical expressions for both natural frequencies and vibration mode shapes. The resulting modal solutions were characterized by nodal circles and nodal diameters, corresponding to radial and circumferential mode indices, respectively. To validate the analytical model, the authors compared the predicted natural frequencies and mode shapes with finite element simulations performed in ANSYS, reporting frequency deviations below 4%.

Furthermore, comparison with experimental measurements from human volunteers demonstrated that observed resonance peaks in the tympanic membrane frequency response arise from the combined contribution of multiple natural modes rather than a single vibration mode. This finding provided important insight into the interpretation of experimental resonance behavior and highlighted the limitations of simplified single-mode assumptions. Although the model neglects certain physiological effects such as tension variation induced by malleus motion, it offers a computationally efficient and physically interpretable framework that serves as a valuable reference for middle ear biomechanics and surgical applications.

B. Modeling Sound Transmission of the Human Middle Ear Using Finite Element [2]

Chen et al. (2013) developed a detailed three-dimensional finite element (FE) model of the human middle ear to investigate sound transmission mechanisms and their clinical implications. The model was reconstructed from high-resolution computed tomography (HRCT) images and included anatomically accurate representations of the tympanic membrane (TM), ossicular chain, external ear canal, tympanic cavity, and mastoid cavity.

A key contribution of this work was the modeling of the tympanic membrane as a three-layer solid structure rather than a shell element, enabling realistic acoustic–structural coupling and allowing pressure differences across the membrane to be captured accurately. The FE model was validated by comparing simulated umbo displacement responses with published temporal-bone experimental measurements, showing good agreement across a wide frequency range.

Using the validated model, the authors investigated clinically relevant variations in middle ear parameters, including changes in tympanic membrane stiffness and thickness as well as alterations in ligament properties. The results demonstrated that increased TM stiffness and thickness significantly reduce umbo and stapes footplate displacement, particularly at low frequencies, which is consistent with clinical observations of reduced sound transmission following chronic inflammation or surgical intervention. Overall, this study highlights the sensitivity of middle ear mechanics to tympanic membrane properties and demonstrates the effectiveness of FE modeling as a tool for understanding middle ear biomechanics and supporting clinical applications.

C. Transient Experimental and Numerical Characterization of Tympanic Membrane Vibration[3]

Garcia-Manrique et al. (2023) proposed a combined experimental and numerical framework to investigate the dynamic behavior of the human tympanic membrane (TM) under transient acoustic excitation. Full-field TM vibrations were measured on human temporal bones using high-speed digital holography, enabling detailed time-domain observation of membrane displacement with high spatial and temporal resolution.

Based on the experimental measurements, a specimen-specific finite element (FE) model of the tympanic membrane was developed. Material properties and damping parameters were iteratively adjusted to ensure close agreement between simulated and experimentally observed transient responses. The validated FE model successfully reproduced spatiotemporal vibration patterns and displacement amplitudes measured experimentally and was subsequently employed to perform modal analysis, revealing a dense distribution of natural frequencies and corresponding mode shapes.

By integrating transient experimental data with finite element modeling, this study provides a realistic and data-driven characterization of tympanic membrane mechanics. The proposed approach complements analytical free-vibration and steady-state numerical models by explicitly accounting for damping effects, boundary conditions, and acoustic–structural coupling. As a result, the work is particularly relevant for clinical and patient-specific investigations of middle ear mechanics and serves as an important experimental validation reference for theoretical and computational tympanic membrane models.

D. Machine Learning Approaches for Audiometry-Based Assessment of Meniere's Disease[4]

Liu et al. (2025) investigated the application of machine learning techniques for the diagnosis of Meniere's disease and the prediction of endolymphatic hydrops using pure-tone audiometry data. Audiometric measurements from a large patient cohort were used to extract frequency-based features and train multiple supervised classification models. Among the evaluated approaches, a Light Gradient Boosting Machine (LightGBM) achieved the highest diagnostic performance, with accuracy comparable to that of expert clinicians.

Although this study does not explicitly model the mechanical behavior of the tympanic membrane or middle ear structures, it demonstrates the effectiveness of data-driven methods in interpreting auditory system dysfunction through measurable hearing outcomes. The work complements biomechanical and numerical models of the ear by providing a clinical machine-learning perspective that may support diagnosis and validation of physics-based auditory models.

III. The free vibration model of the TM

Tympanic membrane, also called as the eardrum, comprises of a membrane body and annular ligament as shown in Figure 1. The annular ligament connects the membrane body and bony tympanic ring, hence fixing the eardrum. The manubrium of malleus embeds in TM from its edge to center. The umbo

is located in the central part. The thickness of TM is between 50 and 100 μm, and the average thickness is 74 μm. The horizontal axis length is 8–9 mm and the vertical axis length is 8.5–10 mm. The total area is 85 mm^2, while the actual area which takes part in the physiological activity is about 55 mm^2.

Therefore, four hypotheses are proposed according to the structural characteristics of TM:

1) The TM is soft and springy, which cannot resist moment, and the tension is in the tangent plane at any time.
2) The malleus vibration caused by TM is a small amplitude vibration. The maximum displacement of the malleus is about 1×10^{-5} mm under the conditions of 100–10,000 Hz sound frequency and 90 dB sound pressure.
3) The influence of TM thickness variation in vibration process can be neglected.
4) The annular ligament is the hinge support of TM.

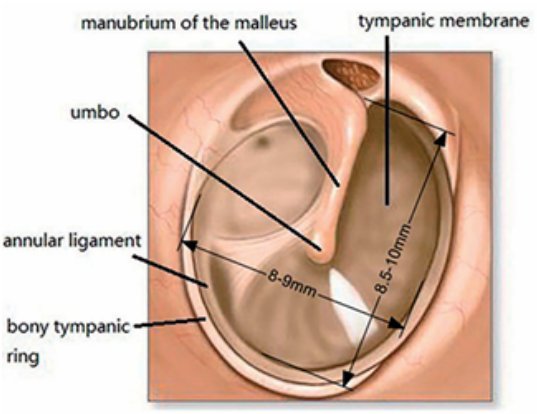

Fig. 1. The TM Structure diagram

According to the above hypotheses, TM can be simplified as a sectorial annulus membrane which cannot resist bending and shear deformation. It completely depends on annular ligament tension to balance the horizontal load. Therefore, TM is set as a completely flexible and constant thickness sheet, subjected to a uniform tension in any direction, in Figure 2(a).

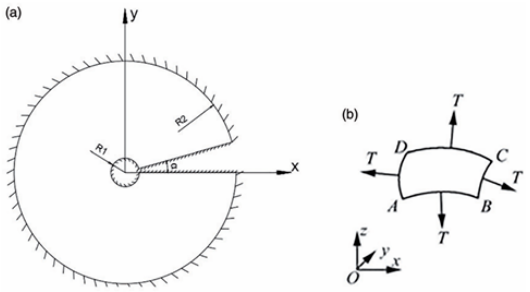

Fig. 2. The Simplified TM Structure

Set up a xoy plane as the TM plane without deformation, z axis being perpendicular to the plane, and constitute a right-handed coordinate system in Figure 2(b). T is the TM tension. d is the thickness of TM. ρ is the quality on the unit area and w is the displacement along the z axis. Suppose the inner diameter of TM is R_1, the outer diameter of TM is R_2, and the angle of sectorial annulus membrane is α.

The geometrical equation of large deformation of the circular membrane in polar coordinates is given by

$$\varepsilon_r = \frac{du_r}{dr} + \frac{1}{2}\left(\frac{dw}{dr}\right)^2 \tag{1}$$

$$\varepsilon_\theta = \frac{u_r}{r} \tag{2}$$

where ε_r represents the radial strain, ε_θ represents the circumferential strain, u_r denotes the radial displacement.

Substituting Equation (2) into Equation (1), the equation of compatibility is

$$\varepsilon_r = \frac{d}{dr}(r\varepsilon_\theta) + \frac{1}{2}\left(\frac{dw}{dr}\right)^2 \tag{3}$$

The physical equations are

$$\varepsilon_r = \frac{1}{E}(\sigma_r - \mu\sigma_\theta) = \frac{1}{Ed}(N_r - \mu N_\theta) \tag{4}$$

$$\varepsilon_\theta = \frac{1}{E}(\sigma_\theta - \mu\sigma_r) = \frac{1}{Ed}(N_\theta - \mu N_r) \tag{5}$$

where E represents Young's modulus; μ represents Poisson's ratio.

Substituting Equation (4) and Equation (5) into Equation (3), yield

$$r^2\frac{d^2}{dr^2}(rN_r) + r\frac{d}{dr}(rN_r) - rN_r = -\frac{1}{2}Ed\left(\frac{dw}{dr}\right)^2 \tag{6}$$

The equation of transverse free vibration of membranes is:

$$\nabla^2 w = \frac{\rho}{T}\frac{\partial^2 w}{\partial t^2} \tag{7}$$

Since the boundary is a circle, we transform Equation (6) to polar coordinates (r, θ):

$$\frac{\partial^2 w}{\partial r^2} + \frac{1}{r}\frac{\partial w}{\partial r} + \frac{1}{r^2}\frac{\partial^2 w}{\partial \theta^2} = \frac{\rho}{T}\frac{\partial^2 w}{\partial t^2} \tag{8}$$

The boundary conditions are as follows:

$$w(R_1, \theta, t) = w(R_2, \theta, t) = 0, \quad w(r, 0, t) = w(r, \alpha, t) = 0 \tag{9}$$

According to variables separation method, let:

$$w(r, \theta, t) = W(r, \theta) \cdot q(t) \tag{10}$$

Substituting Equation (10) into Equation (6), we obtain two differential equations of variable separation:

$$\ddot{q}(t) + \omega^2 q(t) = 0 \tag{11}$$

$$\frac{\partial^2 W}{\partial r^2} + \frac{1}{r}\frac{\partial W}{\partial r} + \frac{1}{r^2}\frac{\partial^2 W}{\partial \theta^2} + \frac{\omega^2\rho}{T}W = 0 \tag{12}$$

where ω is the constant. According to the general solution of differential equation, solution of Equation (11) can be expressed as:

$$q(t) = c_1 \sin(\omega t + \varphi) \tag{13}$$

This means harmonic oscillation that natural frequency is ω. Solve Equation (12) by using the variable separation method, let:

$$W(r,\theta) = L(r) \cdot \Theta(\theta) \tag{14}$$

Substituting Equation (14) into Equation (12), we obtain two differential equations of variable separation:

$$\frac{d^2\Theta}{d\theta^2} + n^2\Theta = 0 \tag{15}$$

$$\frac{r^2}{L}\frac{d^2L}{dr^2} + \frac{r}{L}\frac{dL}{dr} + r^2k^2 = n^2 \tag{16}$$

where

$$k^2 = \omega^2\rho/T \tag{17}$$

Solution of Equation (15) can be calculated as:

$$\Theta(\theta) = c_2\sin(n\theta + \phi) \tag{18}$$

From Equation (9), we get:

$$\Theta(0) = \Theta(\alpha) = 0 \tag{19}$$

Substituting Equation (19) into (18), we obtain:

$$\phi = 0 \tag{20}$$

Let

$$n = k\pi/\alpha \quad (k, n \text{ are integers}) \tag{21}$$

Equation (16) can be transmitted to:

$$r^2\frac{d^2L}{dr^2} + r\frac{dL}{dr} + (r^2k^2 - n^2)L = 0 \tag{22}$$

This is an n-order Bessel equation, the solution is:

$$L(r) = c_3J_n(kr) + c_4Y_n(kr) \tag{23}$$

where $J_n(kr)$ is Bessel function of the first kind, $Y_n(kr)$ is Bessel function of the second kind. They can be expressed as:

$$J_n(kr) = \sum_{m=0}^{\infty}\frac{(-1)^m}{m!\Gamma(n+m+1)}\left(\frac{kr}{2}\right)^{n+2m} \tag{24}$$

$$Y_n(kr) = \lim_{\beta\to n}\frac{J_\beta(kr)\cos\beta\pi - J_{-\beta}(kr)}{\sin\beta\pi} \tag{25}$$

According to boundary conditions that the TM inner and outer edge is fixed, we obtain:

$$\begin{cases} L(R_1) = c_3J_n(kR_1) + c_4Y_n(kR_1) = 0 \\ L(R_2) = c_3J_n(kR_2) + c_4Y_n(kR_2) = 0 \end{cases} \tag{26}$$

If c_3 and c_4 exist as non-zero solutions, then there must be:

$$J_n(kR_1)Y_n(kR_2) - J_n(kR_2)Y_n(kR_1) = 0 \tag{27}$$

Then, $k_m^{(n)}$ for mth zero can be calculated. The natural frequency ω_{mn} is:

$$\omega_{mn} = k_m^{(n)} \cdot \sqrt{T/\rho} \tag{28}$$

The corresponding natural vibration modes are:

$$W_{mn}(r,\theta) = \left[J_n(k_m^{(n)}r) - \frac{J_n(k_m^{(n)}R_2)}{Y_n(k_m^{(n)}R_2)}Y_n(k_m^{(n)}r)\right]\sin\left(\frac{k\pi}{\alpha}\theta\right) \tag{29}$$

Finally, we get the general solution for free vibration of sectorial annulus TM with fixed boundary:

$$w(r,\theta,t) = \sum_{m=1}^{\infty}\sum_{k=1}^{\infty}A_{mn}W_{mn}(r,\theta)\sin(\omega_{mn}t + \varphi) \tag{30}$$

where A_{mn} and φ are determined by initial conditions.

IV. Methodology

This study employs a comprehensive multi-modal approach to model tympanic membrane dynamics, progressing from classical mathematical derivation to numerical methods, deep learning, and finally, clinical simulation. The methodology is divided into four distinct phases: (1) Analytical derivation using Bessel functions as shown in the previous section, (2) Numerical solution using the Finite Difference Method (FDM) in polar coordinates,and (3) Simulation Tool(COMSOL) (4) Physics-Informed Neural Networks (PINNs)

A. Bessel Function (Analytical)

To validate our results, we wrote a Python script that calculates the exact natural frequencies of the eardrum.

- **Model:** The code models the eardrum as an Annular Sector (a ring shape with $R_1 = 0.5$ mm and $R_2 = 4.5$ mm) to account for the malleus attachment, which is more accurate than a simple circle.
- **Method:** We used the `scipy` library to evaluate the characteristic equation, which includes Bessel functions of both the first (J) and second (Y) kinds due to the hole in the center.
- **Solver:** A root-finding algorithm (Brent's method) was used to numerically solve for the wavenumbers (k) that satisfy the boundary conditions.

It efficiently handles sparse Jacobian matrices, optimizing performance for large systems.

B. Finite Difference (Numerical Method)

To verify the analytical results using a different mathematical approach, we implemented a numerical solver in Python.

- **Grid Structure:** Instead of a standard square grid, we created a Polar Grid (defined by radius r and angle θ). This matches the circular shape of the eardrum much better and avoids "stair-step" edges.
- **Discretization:** We used the Central Finite Difference method. This approximates the slope of the membrane at every point by comparing it to its neighbors (left, right, up, down).
- **Matrix Solver:** Unlike simple simulations that run loop-by-loop over time, this code builds a massive "Stiffness Matrix" ($\mathbf{A}$) representing the entire membrane.
- **Eigenvalue Calculation:** We used a linear algebra solver (`scipy.sparse.linalg.eigs`) to compute the Eigenvalues of this matrix.
  - **Result:** This gives us the natural frequencies directly without needing to simulate seconds of vibration, providing a robust cross-check against the Bessel function results.

C. COMSOL Simulation

To validate the analytical and numerical solution, a finite element model was developed using **COMSOL Multiphysics**.

The simulation focused on extracting the natural frequencies and vibration mode shapes of the tympanic membrane, which were later compared with results of the paper A. mentioned in the literature review.

- **Geometry Definition and Physical Properties:** The tympanic membrane was modeled as a two-dimensional sectorial annulus membrane using the same geometric and material parameters as the numerical method. The *Membrane* interface in COMSOL Multiphysics was employed to represent the thin, tension-dominated behavior of the tympanic membrane.
- **Boundary Conditions:** To replicate the anatomical constraints of the tympanic membrane, **fixed boundary conditions** were applied to enforce zero transverse displacement at the edges, matching the analytical boundary conditions used in the theoretical model.
- **Study Type and Solution Method:** An Eigen frequency study was conducted to determine the natural frequencies and corresponding vibration modes of the membrane under free vibration conditions without external excitation. Multiple eigenmodes were extracted to enable direct comparison with analytical results for different radial and circumferential mode numbers.
- **Visualization of Vibration Modes:** Although the model is two-dimensional, the vibration modes were visualized as **three-dimensional deformed surfaces** by mapping the out-of-plane displacement onto the vertical axis, with a scaling factor applied to enhance visibility.
- **Model Validation:**The natural frequencies obtained from the COMSOL simulation were compared with the analytical solution derived using separation of variables and Bessel functions, as well as with ANSYS finite element results reported in the literature. The comparison showed **close agreement, with small deviations** attributed to numerical discretization and stiffness approximation inherent in finite element formulations.
  This confirms the validity of the COMSOL membrane model as an effective numerical tool for studying the free vibration behavior of the human tympanic membrane.

D. PINNS (Machine Learning Implementation)

Physics-Informed Neural Network (PINN) Architecture

We approximate the solution $W(r, \theta)$ using a fully connected Feed-Forward Neural Network (FNN). The network architecture consists of:

- **Input Layer:** 2 neurons (r, θ).
- **Hidden Layers:** 3 layers with 128 neurons each.
- **Activation Function:** `tanh`, chosen for its smooth, non-zero higher-order derivatives required for computing the Laplacian.
- **Output Layer:** 1 neuron (approximated displacement $\hat{W}$).

Hard Constraint of Boundary Conditions: Standard PINNs often include boundary conditions as soft penalty terms in the loss function. However, to improve convergence and accuracy, we encode the boundary conditions directly into the network structure (Hard Constraints). The network output $\mathcal{N}(r, \theta)$ is modified as follows:

$$\hat{W}(r, \theta) = \mathcal{N}(r, \theta) \times (r - R_1)(R_2 - r) \times \sin\left(\frac{n\pi\theta}{\alpha}\right) \quad (31)$$

This ansatz ensures that $\hat{W}$ is exactly zero at $r = R_1$, $r = R_2$, $\theta = 0$, and $\theta = \alpha$ by construction, allowing the optimizer to focus entirely on solving the PDE in the interior of the domain.

Loss Function and Sequential Training

We employ a sequential training strategy to discover multiple vibration modes. For a specific angular mode n and radial mode m, the total loss function $\mathcal{L}$ is defined as:

$$\mathcal{L} = \mathcal{L}_{\text{PDE}} + \mathcal{L}_{\text{norm}} + \lambda_{\text{ortho}}\mathcal{L}_{\text{ortho}} \quad (32)$$

1) **Physics Loss ($\mathcal{L}_{\text{PDE}}$):** Measures the residual of the Helmholtz equation using Automatic Differentiation (AutoGrad) to compute exact derivatives:

$$\mathcal{L}_{\text{PDE}} = \frac{1}{N_c}\sum_{i=1}^{N_c}\left|\nabla^2\hat{W}_i + k_{nm}^2\hat{W}_i\right|^2 \quad (33)$$

2) **Normalization Loss ($\mathcal{L}_{\text{norm}}$):** To prevent the trivial solution ($\hat{W} = 0$), we enforce a non-zero amplitude:

$$\mathcal{L}_{\text{norm}} = (\max|\hat{W}| - 1)^2 \quad (34)$$

3) **Orthogonality Loss ($\mathcal{L}_{\text{ortho}}$):** To ensure the network learns a new mode distinct from previously discovered lower-order modes, we enforce orthogonality:

$$\mathcal{L}_{\text{ortho}} = \sum_{j<m}\left(\frac{1}{N_c}\sum_{i=1}^{N_c}\hat{W}_i^{(m)} \cdot \hat{W}_i^{(j)}\right)^2 \quad (35)$$

where $\hat{W}^{(j)}$ represents the fixed solution of a previously trained radial mode.

Training Protocol

The model is implemented in PyTorch. The domain is sampled using $N_c = 2500$ collocation points drawn from a uniform distribution. We use the Adam optimizer with a learning rate of 10^{-3}. Each mode is trained for 3,000 iterations. The orthogonality weight λ_{ortho} is set to 10.0 to strictly enforce mode separation.

V. ANALYSIS AND COMPREHENSIVE COMPARISON

To verify the validity of the proposed model, a test case is used to calculate the natural frequencies and vibration mode shapes of the tympanic membrane (TM). The material and geometric parameters are chosen based on physiological values reported in the literature and are listed below:

$$R_1 = 0.5\,\text{mm}, \quad R_2 = 4.5\,\text{mm}, \quad d = 0.1\,\text{mm} \tag{36}$$

$$E = 33.4\,\text{N/mm}^2, \quad \rho = 0.00012\,\text{g/mm}^2 \tag{37}$$

$$T = 1.35\,\text{N/mm}^2, \quad \nu = 0.3, \quad \alpha = 340^\circ \tag{38}$$

These parameters are used in the analytical solution, the numerical finite difference method, and the COMSOL Multiphysics simulation to allow a fair comparison between the different approaches.

Comparison of Results

We compare the analytical, numerical,and simulation-based methods used to study the free vibration of the tympanic membrane as shown in Table 3 in next page. The comparison focuses on the natural frequencies, vibration mode shapes, and the physical meaning of the results.

a. Natural Frequency Comparison

Table 1 shows the first six natural frequencies obtained using the analytical solution, the finite difference (FD) method, and COMSOL Multiphysics. Overall, the results from the three methods are in good agreement.

The analytical solution is taken as the reference because it is obtained directly from the governing partial differential equation using mathematical methods. The finite difference method gives frequency values that are close to the analytical results, with relative errors generally less than 5%.

Figure 3 shows the percentage error between the finite difference results and the analytical solution for different vibration modes. The maximum error is about 1.5%, which indicates that the numerical method is accurate. The small differences are mainly due to the limited grid resolution and discretization near the inner and outer boundaries of the membrane.

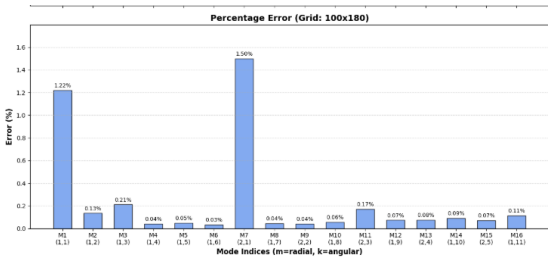

Fig. 3. Percentage Error Difference between analytical and numerical methods

Different vibration modes are presented in the table, where each mode corresponds to a specific vibration pattern of the membrane. The indices $(\mathbf{m}, \mathbf{k})$ describe the radial and circumferential behavior of the mode. Higher modes show more complex vibration patterns and occur at higher natural frequencies.

The results indicate that both the numerical and simulation methods closely match the analytical solution, with maximum errors of $\mathbf{1.6}\%$ and $\mathbf{1.89}\%$, respectively as shown in Table 1.

TABLE I
COMPARISON OF NATURAL FREQUENCIES AND ERROR ANALYSIS

Mode	Analytical (Hz)	Numerical (Hz)	error (%)	COMSOL (Hz)	error (%)
(1,1)	416.46	421.5	1.21	421.55	1.22
(1,2)	471.55	477.73	1.31	477.65	1.29
(1,3)	542.62	550.3	1.42	550.1	1.38
(2,2)	869.28	883.19	1.60	882.6	1.53
(2,3)	951.69	947.03	0.49	946.3	0.57
(3,3)	1352.29	1346	0.47	1343.8	0.63

Overall, the order of the natural frequencies is the same for all three methods. This confirms that the physical behavior of the tympanic membrane is correctly captured by each approach.

b. Machine Learning (PINNs) Results

A PINN approach was employed to compute the vibration modes of a circular membrane, with models trained separately for each angular mode k and radial mode m. The results were compared against reference data, showing close agreement with relative errors ranging from 1.41% to 2.47%. Low-order modes such as $(1,1)$, $(2,1)$, and $(3,1)$ exhibit smaller errors ($\sim$1.4–1.6%), indicating effective capture of fundamental vibration behavior. Higher-order modes like $(1,3)$, $(2,3)$, and $(3,3)$ show slightly higher errors ($\sim$2–2.5%) as shown in Table 2, reflecting increased sensitivity to complex radial variations and potential neural network approximation limitations .

TABLE II
COMPARISON OF NATURAL FREQUENCIES AND ERROR ANALYSIS

Mode	Analytical (Hz)	PINNs (Hz)	error (%)
(1,1)	412.8	421.5	2.11
(2,1)	822.1	840.1	2.19
(3,1)	1228.7	1259.0	2.46
(1,2)	471.1	477.7	1.41
(2,2)	869.3	883.2	1.60
(3,2)	1261.6	1292.7	2.47
(1,3)	541.6	550.3	1.60
(2,3)	929.9	947.0	1.84

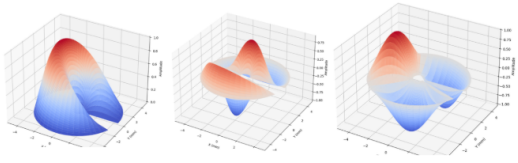

Fig. 4. Visualization of mode(1,1) ,(2,2),and (3,1) using PINNs

TABLE III
COMPARISON OF NATURAL FREQUENCY AND VIBRATION MODES

Modes	Analytical		Numerical		Simulation	
	Freq. (Hz)	Image	Freq. (Hz)	Image	Freq. (Hz)	Image
(1,1)	416.46	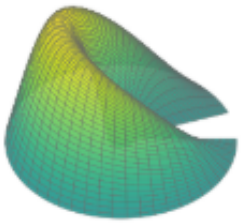	421.5	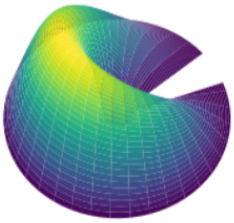	421.55	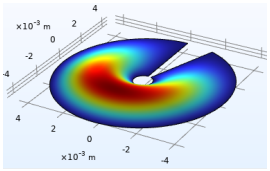
(1,2)	471.12	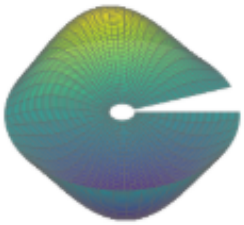	477.65	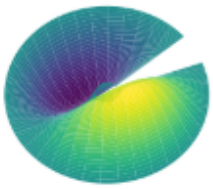	477.73	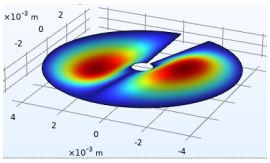
(1,3)	542.62	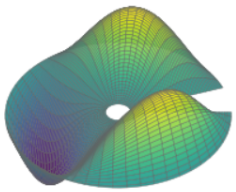	550.1	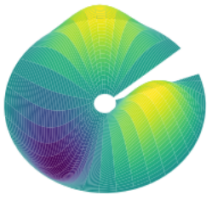	550.3	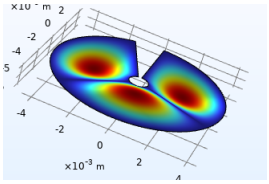
(2,2)	869.28	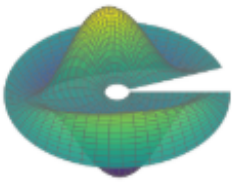	882.6	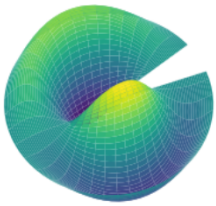	883.19	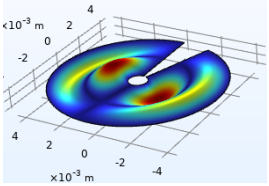
(2,3)	951.69	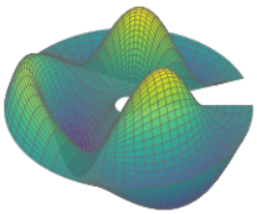	946.3	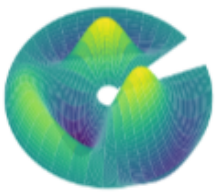	947.03	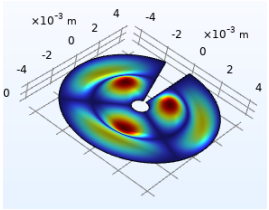
(3,3)	1352.29	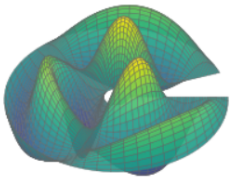	1343.8	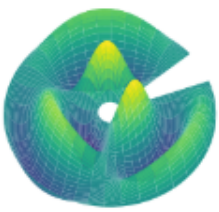	1346	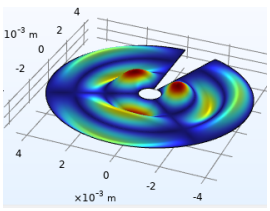

VI. Implemented Applications

A. Machine Learning-Based Diagnostic System

Diagnosing the tension and pathological state of the tympanic membrane based solely on measured frequencies. To address this, a machine learning (ML) classification system was developed to serve as an automated diagnostic tool.

- **Methodology and Dataset Generation:** A synthetic dataset of 2,000 tympanic membrane cases was generated using a physics-based, Bessel-function simulation model. Membranes were classified into flaccid ($T < 30$ N/mm), healthy ($30 \leq T \leq 40$ N/mm), and stiffened ($T > 40$ N/mm) categories. To improve realism and model generalization, 4% Gaussian noise was added to the frequency data.
- **Model Architecture:** Three machine learning models were trained and compared to identify the most robust classifier: a **Random Forest classifier** for capturing nonlinear feature interactions, a **Support Vector Machine (SVM)** for high-dimensional class separation, and a **Multi-Layer Perceptron (MLP)** neural network with ReLU activation and Dropout regularization. For all models, the first six natural eigenfrequencies (f_1–f_6) were used as input features, as they represent the structural vibration signature of the tympanic membrane.
  - **Network Structure as shown in fig(5)**
    - **Input Layer:** Six neurons accepting the first six natural eigenfrequencies (f_1–f_6).
    - **Output Layer:** `Softmax` function outputs normalized probabilities across Healthy, Stiffened, and Flaccid classes.
    - **Activation Function:** `ReLU` in all hidden layers to capture non-linear relationships between frequency modes and membrane tension.

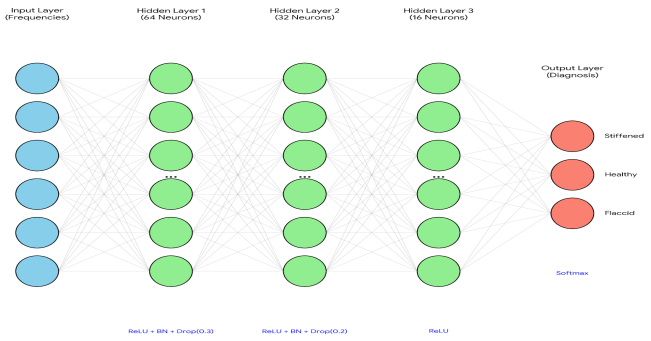

Fig. 5. Simple architecture of the deep neural network classifier.

- **Results and Performance:** The system was evaluated using a testing set (20% of the data) withheld during training. Random Forest and Neural Network models performed best. Key results:
  - **Classification Accuracy:** Achieved $> 98\%$ accuracy for Flaccid, Healthy, and Stiffened membranes.
  - **Confusion Matrix Analysis:** Minimal misclassification, mostly in boundary regions (e.g., "high-normal" misclassified as "stiffened"), which is clinically acceptable.
  - **Regression Capability:** Successfully estimated specific tension values (S_0) with high precision for granular assessment of membrane health.

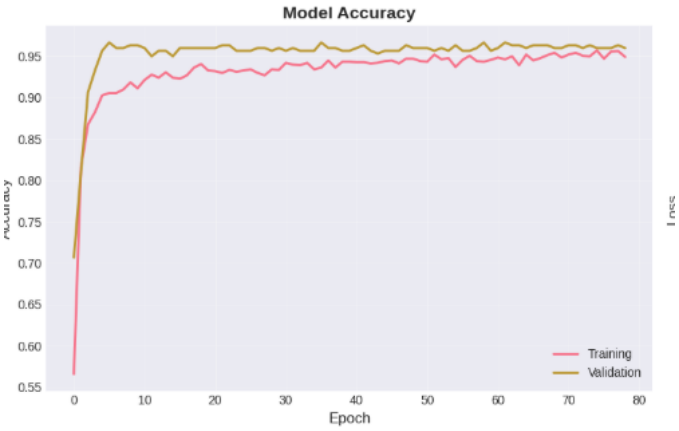

Fig. 6. Neural network training and validation accuracy over 80 epochs

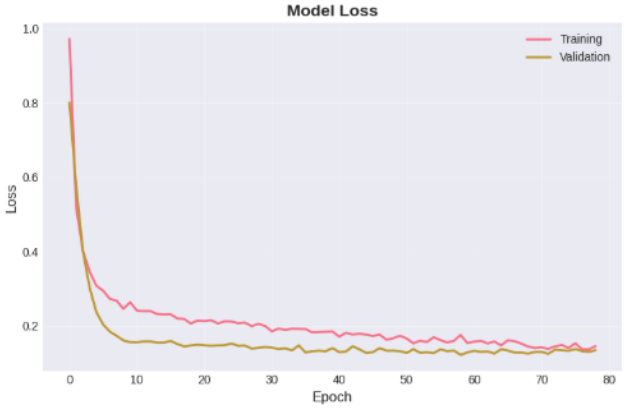

Fig. 7. Neural network training and validation loss over 80 epochs.

B. unity interactive application

To provide a more intuitive understanding of the tympanic membrane (TM) mechanics, we developed a real-time virtual reality (VR) simulation using Unity. The goal was to create an interactive environment where users can visually and physically explore how the TM responds to sound and external forces. This approach not only allows for realistic observation but also enables user-driven experimentation, making complex auditory biomechanics accessible in an engaging way.

1.Vibration Modeling

The core of the simulation is based on an analytical model of TM vibration. Each point on the membrane is displaced according to the following equation:

$$u(r,t) = A \cdot \sin(2\pi f t) \cdot \sin\left(\pi \frac{r}{R}\right) \cdot P(r) \qquad (39)$$

where:

- $u(r,t)$ is the displacement at radial distance r and time t,
- A is the vibration amplitude,
- f is the vibration frequency,
- R is the maximum radius of the membrane,
- $P(r)$ is a pathology factor that reduces displacement in damaged areas ($P(r) = 1$ for healthy tissue and $0 < P(r) \leq 1$ for damaged tissue).

This radial-dependent sinusoidal model approximates the natural mode shapes of the TM and ensures realistic vibration patterns while remaining computationally efficient for real-time VR interaction.

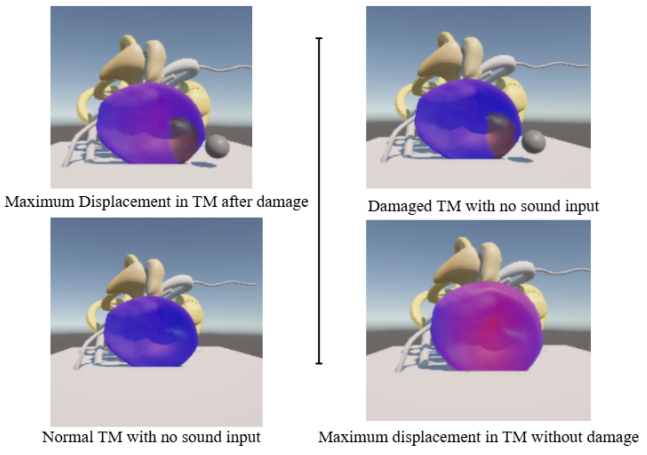

Fig. 8. 4 Modes of Simultation

2.Modeling Damage and Tears

To simulate pathological conditions, the TM can develop localized tears when subjected to excessive pressure. If a user applies a force beyond a defined threshold, the membrane creates a visual hole, altering the local vibration response. The damaged region automatically updates the pathology factor $P(r)$, reducing displacement and simulating the compromised structural integrity. This feature enables exploration of both healthy and injured states, providing insights into how tears affect auditory mechanics.

3.User Interaction

The VR environment allows users to interact directly with the TM using a virtual hand or ball. The membrane responds realistically to contact: gentle touches cause small indentations and vibrations, while higher pressure leads to larger deformation and potential tearing. Displacement is calculated based on the hand's proximity and applied force, creating a lifelike response.

A dynamic color overlay represents the intensity of deformation and damage. Red areas indicate maximum displacement, blue areas remain mostly stationary, and tears appear as transparent holes. This visual feedback provides intuitive understanding of the TM's behavior under different conditions.

4.Surgical Visualization Potential

While TM surgery is currently experience-based, this VR model offers a first step toward an interactive visualization tool that could assist surgeons in training. By combining analytical vibration modeling with responsive user interaction, the simulation can help clinicians better understand membrane behavior and practice subtle manipulations before actual surgery. In future work, this system could evolve into a realistic surgical simulator, allowing surgeons to practice procedures in a safe, controlled, and repeatable environment.

VII. Future Work

Future research directions can extend the present analytical framework in several important ways:

1) **Fluid–Structure Interaction (FSI):** Incorporate coupling between the tympanic membrane (TM) and the surrounding air in the external ear canal and middle ear cavity to investigate the effects of acoustic loading, pressure variations, and sound–structure interaction on membrane vibration characteristics.
2) **Coupling with Ossicular Chain Dynamics:** Extend the model to include the malleus–incus–stapes ossicular chain, enabling analysis of how TM vibration modes transmit mechanical energy through the middle ear and influence sound conduction to the inner ear.
3) **Material Heterogeneity and Anisotropy:** Introduce spatially varying thickness and anisotropic material properties to better represent the layered microstructure and fiber orientation of the TM, improving the biomechanical realism of the model.
4) **Nonlinear and Large-Deformation Effects:** Investigate nonlinear vibration behavior under high sound pressure levels, where the assumptions of linear elasticity and small deflections may no longer be valid, allowing more accurate prediction of TM response in extreme acoustic conditions.
5) **Patient-Specific Modeling:** Utilize medical imaging techniques such as computed tomography (CT) or optical coherence tomography (OCT) to construct subject-specific TM geometries and boundary conditions, supporting personalized diagnosis, treatment planning, and evaluation of surgical outcomes.
6) **Immersive visualization and virtual reality (VR) integration**
   While the current Unity-based model allows interactive visualization and voice-driven interaction, future work will focus on extending the system into a fully immersive virtual reality (VR) environment. This enhancement would support intuitive exploration of vibration modes, improved educational tools, and advanced surgical training simulations.

VIII. Conclusion

This work presented a unified multimodal framework for analyzing the free vibration behavior of the human tympanic membrane (TM) by integrating analytical modeling,

numerical simulation, machine learning, and real-time visualization. The TM was idealized as a sectorial annulus membrane under uniform in-plane tension, leading to a two-dimensional wave equation in polar coordinates. Using separation of variables, the governing equation was reduced to a Bessel differential equation, yielding closed-form expressions for natural frequencies and vibration mode shapes.

The analytical solution was validated through a finite difference method (FDM) implemented on a polar grid and through an independent eigenfrequency analysis using COMSOL Multiphysics. The close agreement in frequency ordering and modal patterns across analytical, numerical, and finite element approaches confirms that the simplified sectorial annulus model captures the dominant free-vibration characteristics of the tympanic membrane.

Beyond classical modeling, a physics-informed neural network (PINN) was introduced as a data-driven solver that embeds the governing partial differential equation and boundary conditions directly into the learning process. In addition, a machine learning–based diagnostic system was developed to classify tympanic membrane conditions using natural frequency features, demonstrating the potential of vibration-based biomarkers for automated assessment of membrane health.

Finally, an interactive Unity-based three-dimensional simulation was implemented to visualize tympanic membrane vibration in real time, enhancing interpretability and enabling intuitive exploration of resonance behavior. Overall, this study demonstrates that analytical theory, numerical discretization, and machine learning can be coherently combined to study tympanic membrane dynamics, providing a solid foundation for future extensions toward patient-specific modeling, clinical diagnostics, and immersive virtual reality–based educational and surgical planning tools.

REFERENCES

[1] C. Wu, Y. Chen, M. S. H. Al-Furjan, J. Ni, and X. Yang, "Free vibration model and theoretical solution of the tympanic membrane," *Computer Assisted Surgery*, vol. 21, pp. 62–69, 2016, doi: 10.1080/24699322.2016.1240315.

[2] J. Garcia-Manrique, C. Furlong, A. Gonzalez-Herrera, and J. T. Cheng, "Numerical model characterization of the sound transmission mechanism in the tympanic membrane from a high-speed digital holographic experiment in transient regime," *Acta Biomaterialia*, vol. 159, pp. 63–73, Mar. 2023, doi: 10.1016/j.actbio.2023.01.048.

[3] P. J. Prendergast, P. Ferris, H. J. Rice, and A. W. Blayney, "3-4; ProQuest Nursing & Allied Health Source pg."

[4] J. Shan, H. Yamazaki, J. Li, and S. Kawano, "Theoretical and experimental study on traveling wave propagation characteristics of artificial basilar membrane," *Scientific Reports*, vol. 15, no. 24041, 2025.

[5] F. De Faveri, F. Ceriani, and W. Marcotti, "In vivo spontaneous Ca2+ activity in the pre-hearing mammalian cochlea," *Nature Communications*, vol. 16, no. 29, 2025.

[6] X. Liu et al., "Applications of Machine Learning in Meniere's Disease Assessment Based on Pure-Tone Audiometry," *Otolaryngology - Head and Neck Surgery (United States)*, vol. 172, no. 1, pp. 233–242, Jan. 2025, doi: 10.1002/ohn.956.

[7] B. D. D. Bjarki, A. S. Axel, K. C. Kaare, et al., "Increasing rate of middle ear ventilation tube insertion in children in Denmark," *Int J Pediatr Otorhinolaryngol*, 2014;79:1541–1544.

[8] V. Vincenzo, M. Francesca, B. Barbara, et al., "Acquired middle ear cholesteatoma in children with cleft palate: experience from 18 surgical cases," *Int J Pediatr Otorhinolaryngol*, 2014;78:918–922.

[9] G. Volandri, F. D. Puccio, P. Forte, et al., "Model-oriented review and multi-body simulation of the ossicular chain of the human middle ear," *Med Eng Phys*, 2012;34:1339–1355.

[10] K. Martin, S. Hannes, H. Alexander, et al., "Influence of the middle ear anatomy on the performance of a membrane sensor in the incudostapedial joint gap," *Hear Res*, 2013;301:35–43.

[11] S. I. Chen, M. H. Lee, C. M. Yao, et al., "Modeling sound transmission of human middle ear and its clinical applications using finite element analysis," *Kaohsiung J Med Sci*, 2013;29:133–139.

[12] F. Mattia, "Virtual middle ear: A dynamic mathematical model based on the finite element method," Ph.D. dissertation, Swiss Federal Institute of Technology, Mendrisio, 2003.

[13] T. Koike, H. Wada, and T. Kobayashi, "Modeling of the human middle ear using the finite-element method," *J Acoust Soc Am*, 2002;111:1306–1317.

[14] R. Z. Gan, Q. Sun, and R. K. Drer Jr., et al., "Three-dimensional modeling of middle ear biomechanics and its applications," *Otol Neurotol*, 2002;23:271–280.

[15] H. G. Liu, N. Ta, and Z. S. Rao, "Numerical modeling of human middle ear biomechanics using finite element method," *J Donghua Univ*, 2011;28:115–118.

[16] W. J. Yao, W. Li, L. J. Fu, et al., "Numerical simulation and transmitting vibration analysis for middle-ear structure," *J Syst Simul*, 2009;21:651–654.

[17] J. P. Vard, D. J. Kelly, A. W. Blayney, et al., "The influence of ventilation tube design on the magnitude of stress imposed at the implant/tympanic membrane interface," *Med Eng Phys*, 2008;30:154–163.

[18] R. Z. Gan, Q. Sun, B. Feng, et al., "Acoustic-structural coupled finite element analysis for sound transmission in human ear-pressure distributions," *Med Eng Phys*, 2006;28:395–404.

[19] A. Venkatesh, K. Joseph, D. Carlie, et al., "Effects of ear canal static pressure on the dynamic behavior of outer and middle ear in newborns," *Int J Pediatr Otorhinolaryngol*, 2016;82:64–72.

[20] M. A. Brown, X. D. Ji, and R. Z. Gan, "3D Finite Element Modeling of Blast Wave Transmission from the External Ear to Cochlea," *Annals of Biomedical Engineering*, vol. 49, pp. 757–768, 2021.